*mathematics*

MDPI

*Article*

# The Basic Reproduction Number and Delayed Action of T Cells for Patients Infected with SARS-CoV-2

**Yingdong Yin [1], Yupeng Xi [1], Cheng Xu [1] and Qiwen Sun [2,*]**

[1] School of Mathematics and Information Science, Guangzhou University, Guangzhou 510006, China; yydyyds@sina.com (Y.Y.); 201123xyp@sina.com (Y.X.); xc203520@sina.com (C.X.)
[2] Guangzhou Center for Applied Mathematics, Guangzhou University, Guangzhou 510006, China
* Correspondence: qwsun@gzhu.edu.cn

**Abstract:** COVID-19 has been prevalent for the last two years. The transmission capacity of SARS-CoV-2 differs under the influence of different epidemic prevention policies, making it difficult to measure the infectivity of the virus itself. In order to evaluate the infectivity of SARS-CoV-2 in patients with different diseases, we constructed a viral kinetic model by adding the effects of T cells and antibodies. To analyze and compare the delay time of T cell action in patients with different symptoms, we constructed a delay differential equation model. Through the first model, we found that the basic reproduction number of severe patients is greater than that of mild patients, and accordingly, we constructed classification criteria for severe and mild patients. Through the second model, we found that the delay time of T cell action in severe patients is much longer than that in mild patients, and accordingly, we present suggestions for the prevention, diagnosis, and treatment of different patients.

**Keywords:** viral kinetic model; SARS-CoV-2; basic reproduction number; the delay time of T cells action

**MSC:** 34K05; 92C37; 92C40



**Citation:** Yin, Y.; Xi, Y.; Xu, C.; Sun, Q. The Basic Reproduction Number and Delayed Action of T Cells for Patients Infected with SARS-CoV-2. *Mathematics* **2022**, *10*, 2017. https://doi.org/10.3390/ math10122017

Academic Editor: Jia Li

Received: 9 May 2022
Accepted: 9 June 2022
Published: 11 June 2022



## 1. Introduction

The COVID-19 pandemic has lasted for two years, with over 526 million confirmed cases and over 6 million deaths globally as of 29 May 2022 [1]. Clinically, patients with mild and moderate disease often have mild clinical symptoms, while severe patients may experience shortness of breath or even lung failure [2]. Compared with patients with mild symptoms, those with severe symptoms have a stronger inflammatory innate immunity response, often accompanied by a cytokine storm, which is also one of the main factors leading to death caused by COVID-19 [3]. In terms of adaptive immunity, it takes more time for effector T cells and B cells to fully mature in patients with severe disease [4], and B cells can generate specific IgM and IgG to neutralize viruses [5].

The viral kinetic model is a dynamic model that describes the dynamic process of viral infection in the body. Nowak et al. [6] developed a dynamic model to study the dynamic process of HBV infection in the human body, which is considered the basic model of viral infection dynamics [7]. The simplest viral kinetic model consists of only three populations: the target cells, the infected cells, and free viruses [8], and more populations can be added according to the research needs. For example, Baccam et al. [9] added an eclipse phase, which refers to cells that have been infected but have not produced the viruses. Jiao et al. [10] added CD4+ T cells based on the characteristics of HIV infection.

In order to study the effect of adaptive immunity on infection, Miao et al. [11] took antibodies and CD8+T cells into consideration. Nowak et al. [12] and Rong et al. [13] categorized free virus populations into drug-resistant and non drug-resistant viruses to study the virulence of drugs against viruses. Pawelek et al. [14] considered the effect of

interferons in the early stage of viral infection to gain insight into the antiviral effect of innate immunity.

The basic reproduction number represents the average number of infected individuals that an infected individual can produce. If $R_0$ is greater than 1, the infection will spread. In the early stage of the epidemic, a large number of studies calculated the basic reproduction number for COVID-19's transmission through the transmission dynamics model. The overview of Alimohamadi et al. [15] can be referred to for details. Affected by the epidemic prevention and control mechanisms employed by various countries, the basic reproduction number of transmission may not reflect the infectivity of the virus itself, in which case the calculation of the basic reproduction number based on the viral kinetic model has an advantage in terms of reflecting the infectivity of the virus.

By using the basic virus kinetic model and changes in the viral load in experimental animals, Goncalves et al. [16] calculated the basic reproduction number $R_0$. Further, Rodriguez et al. [17] analyzed the difference in $R_0$ between young and old experimental animals. Different from the previous two studies, Vaidya et al. [18] calculated the basic reproduction number of different ferrets with the aid of a viral kinetic model with drug treatment, and concluded that the average basic reproduction number of SARS-CoV-2 is 2.05.

Simple models are convenient for calculation; however, more complex models are required to describe more complex immune responses. With the development of studies on the infection mechanism of SARS-CoV-2, the viral kinetic model is becoming increasingly complex. For example, in the early stage of COVID-19, Wang et al. [19] took CD8+T cells into account in a model and assumed that SARS-CoV-2 could infect CD8+T, despite there being insufficient evidence for this assumption. Goyal et al. [20] added the effect of inflammatory macrophages on viral infection and damage to healthy cells. Further, Jenner et al. [21] constructed a detailed model to describe the inhibitory effect of immune cells on viral infection, the damage done by cytokines to the body, and the delayed response of T cells. However, none of these models that describe immune responses in detail involve the calculation of the infectivity of the virus—in other words, the basic reproduction number $R_0$. In addition, these studies did not perform a differential analysis between patients with mild and severe disease using the basic reproduction number.

The delay in T-cell action differs significantly between patients with different symptoms [4]. Jenner et al.'s [21] construct for the delay in T-cell action does not consider the variability between patients with mild and severe disease. Goyal et al. [20] found that the use of moderately potent drugs before the onset of peak virus symptoms may cause the body to develop drug resistance. Rodríguez et al. [22] developed a model to study immune cell action in neocrown infections and showed that low clearance of CD8+T cells exacerbates the disease. Néant et al. [23] found that if virus production could be reduced by 90% at the time of admission, the time to virus clearance would be reduced by 2.0–2.9 days. So far, no studies have attempted to determine treatment regimens based on the T-cell content.

The formation of a distinction between mild and severe patients that does not depend on the patient's symptoms could be used to better protect mild cases that are prone to turning severe. Finding an indicator to determine a patient's optimal medication time would also be of great clinical benefit. In this regard, this paper forms preliminary methods.

The rest of this paper is arranged as follows. In Section 2, first and foremost, data sources and processing are explained in detail. Additionally, we construct two viral kinetic models that consider the effects of T cells and antibodies. One model is used to calculate the basic reproduction number $R_0$ (Model 1), and the other model is used to analyze the T cell delay in viral infection (Model 2). Both models consider the effects of T cells and antibodies. The difference is that we regard T cells as having a known dominant function in Model 1, but Model 2 uses a delay differential equation. Finally, the method of parameter estimation and the tools used are introduced in detail. In Section 3, this paper theoretically distinguishes between patients with mild symptoms and others with severe symptoms using real data fit the model. Additionally, the difference in viral infection in patients with

mild or severe symptoms is analyzed. In practice, this paper can provide patients with classification criteria based on the basic reproduction number and can be used as a basis for diagnosis and treatment suggestions.

## 2. Methods

### *2.1. Patient Classification*

According to The COVID-19 pneumonia diagnosis and treatment scheme of the People's Republic of China (trial version 9) [24], the severity of a patient's condition can be classified into 4 types: mild, moderate, severe, and critical. Compared with mild and moderate types, patients with the severe and critical types show shortness of breath or even respiratory failure. Therefore, clinical classification is simplified by using this standard. In this study, the mild and moderate types are regarded as mild and the severe and critical types as severe.

### *2.2. Data*

The data used in this study were obtained from different studies, but these data are only presented in the form of pictures in these papers, and there are no accurate data tables available. We used WebPlotDigitizer (https://automeris.io/WebPlotDigitizer/, accessed on 13 April 2022) to extract data from the pictures in the main text or supplementary materials. Finally, we analyzed and processed these data for use in our study.

#### 2.2.1. Viral Load

The viral load can be used to describe the viral content in humans. Different studies have selected different units, and $\log_{10}$(copies/mL) and $10^9$ copies/mL are used as the main units of viral load in this paper. A previous study provided time-varying data on the viral load in 21 mild and 10 severe patients [25]. To ensure the accuracy of image data acquisition, only four patients were selected from each.

Since the selected viral load data was in units of ΔCt ($Ct_{sample} - Ct_{ref}$), we used Figure 2D from [26] which gives the relationship between N1 Ct and ΔCt. We assumed that N1 Ct is not different from the Ct values in other studies. After calculation, $Ct_{ref} = 25$, so Ct = ΔCt + 25. Li K et al. [27] stated that the Ct values of 33 and 28 are equivalent to 4.34 $\log_{10}$(copies/mL) and 5.83 $\log_{10}$(copies/mL), respectively. Similar to the practice in [28], we constructed a linear relationship between the Ct value and $\log_{10}$(copies/mL): 1 $\log_{10}$(copies/mL) = $-0.298 \times$ (1 Ct) $+$ 14.7. After injecting SARS-CoV-2 into volunteers, Killingley et al. [29] found that symptoms appeared 2–4 days after the injection. The selected data were recorded after the onset of symptoms. We assumed that symptoms appeared 2 days after these patients were infected with the virus.

#### 2.2.2. T Cells and Antibodies

For T cells, only CD8+T cells were selected for consideration in this paper. These are immune cells with a killing effect on infected cells. We selected CD8+T, IgM, and IgG data from Figure 3 in [30]. These data were obtained from a study of 707 patients, and statistics on patients with moderate, severe, and critical disease were calculated. For convenience, we used the data of the moderate and critical types. This selection method is reasonable, because patients with moderate disease do not experience respiratory failure, while critical patients do, which is consistent with the distinction standard between mild and severe patients in this study.

### *2.3. Models*

In this section, we describe the construction of two mathematical models. The first model was used to estimate the basic reproduction number of viruses, and the second was used to estimate the start time of T cells. The simple immunological mechanism employed in these two models is shown in Figure 1. Uninfected cells transition to the eclipse phase after being infected, but the virus is not produced. After a period of time, cells become

completely infected and can be recognized by T cells, which can produce free viruses. Free viruses can be neutralized by antibodies.

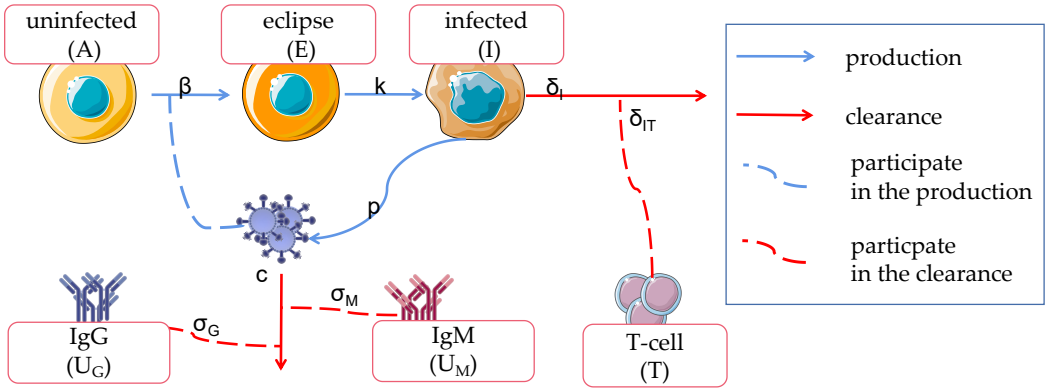


**Figure 1.** Viral infection and immune response diagram. 'Production' means conversion between cells or cell cleavage to produce viruses; 'Clearance' means virus inactivation or cell death; 'Participate in the production' refers to viral infection; 'Participate in the clearance' includes the role of antibodies against the virus and T cell-induced apoptosis in infected cells.

Rodriguez et al. [17] used the basic virus model to estimate the basic reproduction numbers of young and old cynomolgus macaques. The basic virus kinetic model did not add the effects of T cells and antibodies. In this paper, Model 1 ((1)–(4)) reflects the role of T cells and antibodies,

$$\frac{dA}{dt} = \lambda_A \left(1 - \frac{A+E+I}{A_{\max}}\right) A - \beta AV, \tag{1}$$

$$\frac{dE}{dt} = \beta AV - kE, \tag{2}$$

$$\frac{dI}{dt} = kE - \delta_I I - \delta_{IT} I T(t), \tag{3}$$

$$\frac{dV}{dt} = pI - cV - \sigma_M V U_M(t) - \sigma_G V U_G(t). \tag{4}$$

On the basis of Model 1, we construct a delay differential equation Model 2 ((1)–(5)) to study the delay response of T cells:

$$\frac{dT}{dt} = \omega I(t-\tau) - \delta_T T. \tag{5}$$

In these two models, $A$ is the target cells of the virus, i.e., the uninfected cells. Similar to Jenner et al. [21], we assumed that uninfected cells follow the logistic growth law. Both $E$ and $I$ represent cells that have been infected. $E$ is the eclipse phase cells, and $I$ is the completely infected cells, which can lyse to produce viruses. $T(t)$, $U_G(t)$, and $U_M(t)$ represent T cells, IgG, and IgM, respectively. After exposure to the virus, healthy cells are transformed into cells in the eclipse phase at the rate $\beta$, and after $1/k$ days, they become completely infected. Infected cells decrease at a certain rate ($\delta_I$) due to NK cell killing or other immune functions and are also induced to undergo apoptosis by T cells after T cells are produced. Free viruses can be produced by infected cells at a rate $p$, which can be reduced due to the effect of antibodies or other immune functions, such as complements. In Model 1, similar to [11], $T(t)$, $U_G(t)$, and $U_M(t)$ are regarded as known time-dependent functions. In Model 2, the assumption of $T(t)$ is removed. In addition, because of the growth and development of T cells, they are assumed to be produced after $\tau$ day. The meanings of all variables and parameters are shown in Table 1:

**Table 1.** The variables and the parameters in the Model 1 and Model 2.

| | |
|---|---|
| $A$ | Uninfected cells ($10^9$ cells/mL) |
| $E$ | Eclipse phase cells ($10^9$ cells/mL) |
| $I$ | Completely infected cells ($10^9$ cells/mL) |
| $V$ | Free virus ($10^9$ copies/mL) |
| $T$ | CD8+T cells ($10^9$ cells/mL) |
| $U_M$ | Antibody IgM (AU/mL) |
| $U_G$ | Antibody IgG (AU/mL) |
| $A_{\max}$ | maximum uninfected cells ($10^9$ cells/mL) |
| $\lambda_A$ | the production rate of uninfected cells (1/day) |
| $\beta$ | the infection rate of uninfected cells (($10^9$ copies/mL)$^{-1}$(1/day)) |
| $k$ | the transition rate from the eclipse phase cells (1/day) |
| $I$ | the death rate of completely infected cells (1/day) |
| $\delta_{IT}$ | the death rate of infected cells by T cells killing (($10^9$ cells/mL)$^{-1}$(1/day)) |
| $p$ | the production rate of virus (1/day) |
| $c$ | the death rate of free virus (1/day) |
| $\sigma_M$ | the death rate of free virus by IgM neutralizing (($10^9$ copies/mL)$^{-1}$(1/day)) |
| $\sigma_G$ | the death rate of free virus by IgG neutralizing (($10^9$ copies/mL)$^{-1}$(1/day)) |
| $\omega$ | the production rate of T cells by completely infected cells recruiting (1/day) |
| $\tau$ | the delay time of T cells (day) |
| $\delta_T$ | the death rate of T cells (1/day) |

The basic reproduction number $R_0$ represents the average number of infected cells that can be generated by infected cells. In order to calculate $R_0$, some studies have assumed that $V$ is proportional to $I$ and have shown that the actual value of $dV/dt$ is very tiny [31,32], approximately equal to 0. Similarly, using their method, we assumed $V = pI/(c + \sigma_M U_M + \sigma_G U_G)$ and substituted it into (4) to simplify it into the following differential equation group ((6)–(8)):

$$\frac{dE}{dt} = \frac{\beta pAI}{c + \sigma_M U_M + \sigma_G U_G} - kE, \tag{6}$$

$$\frac{dI}{dt} = kE - \delta_I I - \delta_{IT} IT, \tag{7}$$

$$\frac{dA}{dt} = \lambda_A \left(1 - \frac{A + E + I}{A_{\max}}\right) A - \frac{\beta pAI}{c + \sigma_M U_M + \sigma_G U_G}. \tag{8}$$

Using the method in [33], we calculated the basic reproduction number $R_0$:

Firstly, we needed to calculate the disease-free equilibrium (DFE) $X_0 = [A_0, E_0, I_0, T_0, U_{G_0}, U_{M_0}]$, where $A_0 = A(0)$, and the following equations are satisfied ((9)–(11)):

$$0 = \frac{\beta pA_0 I_0}{c + \sigma_M U_{M_0} + \sigma_G U_{G_0}} - kE_0, \tag{9}$$

$$0 = kE_0 - \delta_I I_0 - \delta_{IT} I_0 T_0, \tag{10}$$

$$0 = \lambda_A \left(1 - \frac{A_0 + E_0 + I_0}{A_{\max}}\right) A_0 - \frac{\beta pA_0 I_0}{c + \sigma_M U_{M_0} + \sigma_G U_{G_0}}. \tag{11}$$

Secondly, we needed to distinguish between the source and clearance in the infected cell population, that is, the following vector function $\gamma$, $v$, and we solved the differential $D\gamma$, $Dv$:

$$\gamma(E, I) = \begin{pmatrix} \beta pAI/(c + \sigma_M U_M + \sigma_G U_G) \\ kE \end{pmatrix}, v(E, I) = \begin{pmatrix} kE \\ \delta_I I + \delta_{IT} IT \end{pmatrix}, \tag{12}$$

$$F = D\gamma = \begin{pmatrix} 0 & \beta pA/(c + \sigma_M U_M + \sigma_G U_G) \\ k & 0 \end{pmatrix}, V = Dv = \begin{pmatrix} k & 0 \\ 0 & \delta_I + \delta_{IT} T \end{pmatrix}. \quad (13)$$

Finally, the DFE was substituted into (13), and the basic reproduction number was calculated by $R_0 = \rho(FV^{-1}|_{X_0})$, where $\rho(A)$ means the spectral radius of matrix $A$ and $FV^{-1}$ is called the next generation matrix. DFE is locally asymptotically stable if $R_0 < 1$ but unstable if $R_0 > 1$ [33]. We calculated $R_0$ as follows:

$$R_0 = \sqrt{\frac{\beta p A_0}{(c + \sigma_M U_{M_0} + \sigma_G U_{G_0})(\delta_I + \delta_{IT} T_0)}}. \quad (14)$$

### *2.4. Data Fitting and Parameter Estimation*

In order to reduce the number of free parameters, this study referred to other similar studies to determine the estimates of some parameters and DFE, as shown in Table 2:

**Table 2.** The variables and parameters in Model 1 and Model 2.

| | | | |
|---|---|---|---|
| $A_0$ | $A(0)$ | 0.16 | Reference [21] |
| $E_0$ | $E(0)$ | 0 | Directed estimate |
| $I_0$ | $I(0)$ | 0 | Directed estimate |
| $T_0$ | $T(0)$ | $1.1 \times 10^{-4}$ | Reference [21] |
| $U_{M_0}$ | 25 (mild patients) | 15 (severe patients) | Reference [30] |
| $U_{G_0}$ | 40 (mild patients) | 35 (severe patients) | Reference [30] |
| $U_M(0)$ | | 0 | Directed estimate |
| $U_G(0)$ | | 0 | Directed estimate |
| $A_{\max}$ | | 0.16 | Directed estimate |
| $\lambda_A$ | | 0.74 | Reference [21] |
| $k$ | | 3 | Reference [17] |
| $\delta_{IT}$ | | 238 | Reference [21] |

'Directed estimate' refers to the reasonable assumptions given in this paper based on the general viral dynamics model. Before viral infection, the infected cell (E,I) content should be 0, and the antibodies against the SARS-CoV-2 have not been secreted. In addition, we assumed that the maximum growth rate of healthy cells is the initial state.

For Model 1, we first estimate the parameters $\sigma_M$ and $\sigma_G$. For (4), we regard $pI$ as the time-varying parameter varying in Model 1, that is, $pI = a(t)$ and express it as the form of polynomial of order $r$, then (4) can be simplified as follows:

$$\begin{aligned} Y(t) &= \frac{dV}{dt} + cV \\ &= a(t) - \sigma_M X_M(t) - \sigma_G X_G(t) \\ &= a_0 + a_1 t + \cdots + a_r t^r + (-\sigma_M) X_M(t) + (-\sigma_G) X_G(t), \end{aligned} \quad (15)$$

where $a_0, a_1, \cdots, a_r$ denote the coefficient of the polynomial, $X_M(t) = V(t)U_M(t)$, $X_G(t) = V(t)U_G(t)$. If there is an n-dimensional time vector $t = [t_1, t_2, t_3, t_4]$, (15) can be transformed into the following linear regression equation:

$$\begin{bmatrix} Y(t_1) \\ Y(t_2) \\ \vdots \\ Y(t_n) \end{bmatrix} = \begin{bmatrix} 1 & t_1 & \cdots & t_1^r & X_M(t_1) & X_G(t_1) \\ 1 & t_2 & \cdots & t_2^r & X_M(t_2) & X_G(t_2) \\ \vdots & \vdots & & \vdots & \vdots & \vdots \\ 1 & t_n & \cdots & t_n^r & X_M(t_n) & X_G(t_n) \end{bmatrix} \begin{bmatrix} a_0 \\ \vdots \\ a_r \\ (-\sigma_M) \\ (-\sigma_G) \end{bmatrix}, \quad (16)$$

where $\{Y(t_i) = dV(t_i)/dt + cV(t_i) | i = 1, 2, \cdots, n\}$ is the dependent variable and $\{t_{ik}, X_M(t_i), X_G(t_i) \ | k = 1, 2, \cdots, r; i = 1, 2, \cdots, n\}$ is the independent variable. If regression Equation (16) is solved, the specific value of $Y(t_i)$ needs to be calculated. According to the two-stage local polynomial estimation method used in the time-varying parameter estimation [34],

we used the local polynomial estimation to fit $V(t)$. For a specific time node $t_0$, the points in its neighborhood can have the following q-order polynomial based on Taylor expansion:

$$V(t) \approx \beta_0(t_0) + \beta_1(t_0)(t - t_0) + \cdots \beta_q(t_0)(t - t_0)^q.$$

The coefficient estimates are as follows:

$$\hat{\beta}(t_0) = \left(\beta_0(t_0), \beta_1(t_0), \cdots, \beta_q(t_0)\right)^T = \left(X_q^T W_1 X_q\right)^{-1} X_q W_1 Y_V,$$

$$X_q = \begin{bmatrix} 1 & t_1 - t_0 & \cdots & (t_1 - t_0)^q \\ \vdots & \vdots & & \vdots \\ 1 & t_n - t_0 & \cdots & (t_n - t_0)^q \end{bmatrix}, W_1 = \begin{bmatrix} K_{h_1}(t_1 - t_0) & & \\ & \ddots & \\ & & K_{h_1}(t_n - t_0) \end{bmatrix},$$

$$Y_V = [V(t_1), V(t_2), \cdots, V(t_n)]^T.$$

where $K_{h_1}(t) = K(t/h_1)/h_1$, $K(t)$ is the kernel function, and $h_1$ is the bandwidth. Obviously, there can be $dV(t_0)/dt$ and $V(t_0)$ estimates:

$$\hat{V}(t_0) = \beta_0(t_0), \qquad \frac{dV(t_0)}{dt} = \beta_1(t_0).$$

According to the above, we simplified the estimation problem of $\sigma_G$ and $\sigma_M$ into the linear regression problem with constraints ($\sigma_G, \sigma_M > 0$), and the least square method can be used to solve it.

For the other parameters in Model 1, we chose the sum of residual squares of the viral load ($V$) as the minimization objective function ($RSS_V$) and used genetic algorithm, simulated annealing algorithm, and nonlinear least squares method to estimate the parameters.

For Model 2, the estimated values of the same parameters are given based on the estimated parameters in Model 1. For the estimation of $\tau$ and $\omega$, $\delta_T$, the T cell ($T$) residual sum of squares ($RSS_T$) was used to minimize the objective function to estimate these parameters.

$$RSS_V = \sum_{i=1}^{n} \left\{\log_{10}\left(\hat{V}(t_i)\right) - \log_{10}(\bar{V}(t_i))\right\},$$

$$RSS_T = \sum_{i=1}^{n} \left\{\hat{T}(t_i) - \bar{T}(t_i)\right\},$$

where $\hat{V}(t_i)$ and $\bar{V}(t_i)$ represent the estimated value and actual value, respectively, of viral load on day $t_i$ in copies/mL; $\hat{T}(t_i)$ and $\bar{T}(t_i)$ represent the estimated and actual T cell concentrations on day $t_i$, respectively, in $10^9$ cells/mL.

In order to determine the distribution of each parameter and evaluate the distribution difference of each parameter between different diseases, we calculated the distribution of the estimated parameters. However, existing studies provided less viral load data to distinguish between severe and mild patients, resulting in a smaller data sample being selected in this paper. In order to solve this problem, this study used a bootstrap sampling method to estimate the statistical distribution of each parameter. In addition, the solver ode23s and dde23 in Matlab2021a were used to solve ((1)–(5)).

## 3. Results

### *3.1. Basic Reproduction Number and Patient Classification Method*

We used the cube spline interpolation method to smooth $T(t)$, $U_M(t)$, and $U_G(t)$ data, and data with values of less than 0 were expressed as 0. The change in T cells was relatively stable. At the same time, the results from mild patients were obviously higher than those from the severe patients. The amount of antibodies will change significantly after two weeks, as shown in the Figure 2.

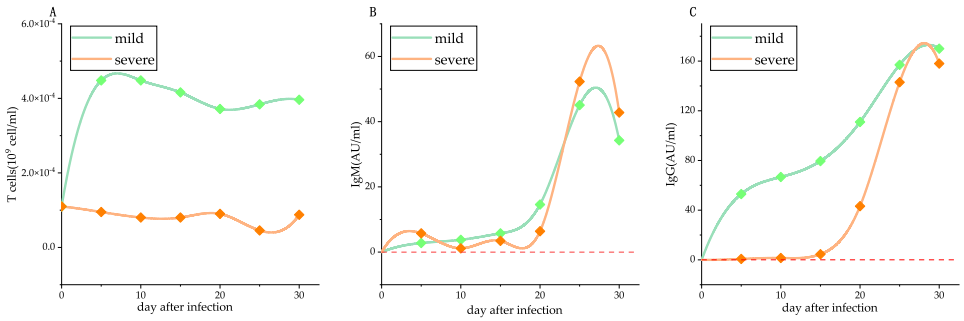


**Figure 2.** (**A**) Dynamic changes of T cells over time; (**B**) Dynamic changes of IgM over time; (**C**) Dynamic changes of IgG over time. In this paper, the initial value of T cells is treated as [21], and the initial values of IgM and IgG are treated as 0. Other data are from [30].

The study presented in [29] on symptoms of COVID-19 and the immune response provided information on the dynamic change in viral load used for data fitting. The volunteers were young adults aged between 20 and 29 years old with mild symptoms, so we used the data from mild patients and the dynamic process presented in [30]. With the method described earlier, we used the Epanechnikov function (17) as the kernel function for the local estimated polynomial, from which we selected bandwidth 5 and determined the polynomial order to be 4,

$$K(x) = \begin{cases} 0.75(1-x^2), & \text{if } |x| \leq 1, \\ 0, & \text{otherwise.} \end{cases} \tag{17}$$

The fitting results are shown in Figure 3. For the estimate of $V(t)$, refer to the curve shown in Figure 3A. To clearly show the degree of fit between the fitting data and the original data, we constructed Figure 3B, because the units of the original data were $\log_{10}$(copies/mL).

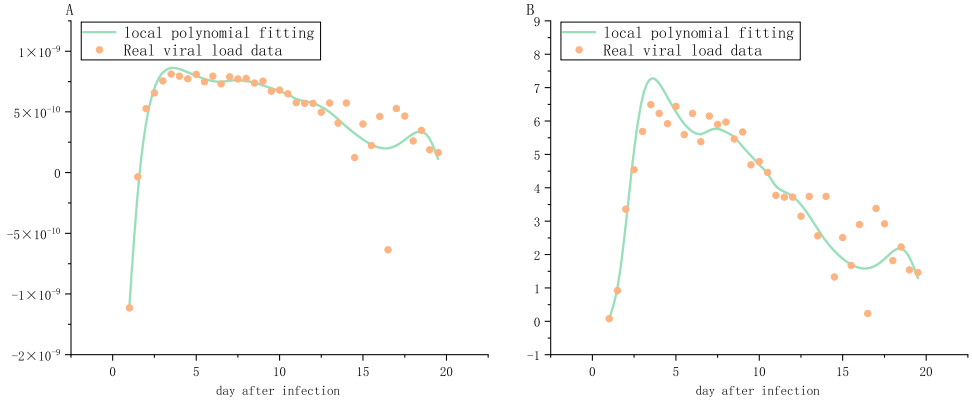


**Figure 3.** Fitting viral load data using local polynomial estimation. (**A**) Unit: $10^9$ copies/mL; (**B**) Unit: $\log_{10}$(copies/mL).

Based on the method defined in Section 2.4, we defined c = 1.81 [21] with final estimates of $\sigma_G = 0.0042$ and $\sigma_M = 0.0372$. Furthermore, we assumed that the two parameters of severe disease patients and mild disease patients were consistent.

After fitting Model 1 ((1)–(4)) with the viral loads of mild and severe patients, the estimated parameters and basic reproduction number were obtained, as shown in Table 3, and the model fitting details are shown in Figure 4. The peak viral load of SARS-CoV-2 was shown to occur in the first week [35], which is consistent with the results shown the model in this paper. As shown in Table 3, the basic reproduction numbers of the 4 mild patients were 2.48, 1.85, 2.46, and 2.29 with an average basic reproduction number of 2.27, and the basic reproduction numbers of the four severe patients were 4.13, 2.79, 3.06, and 2.81 with

an average basic reproduction number of 3.20. An $R_0$ value of greater than 1 indicates that the viral infection will continue to develop, and an $R_0$ value of less than 1 indicates that the viral infection will disappear, which suggests that regardless of whether symptoms are mild or severe, the eight patients will all require drug treatment to control the spread of the virus in vivo. Additionally, $R_0$ can be used to test the medicine's efficacy or the effect of a vaccine on patients [18]. The severe disease patients require an efficacy rate of 68.75%, and the mild ones require an efficacy rate of 55.94%, on average $((R_0 - 1)/R_0)$.

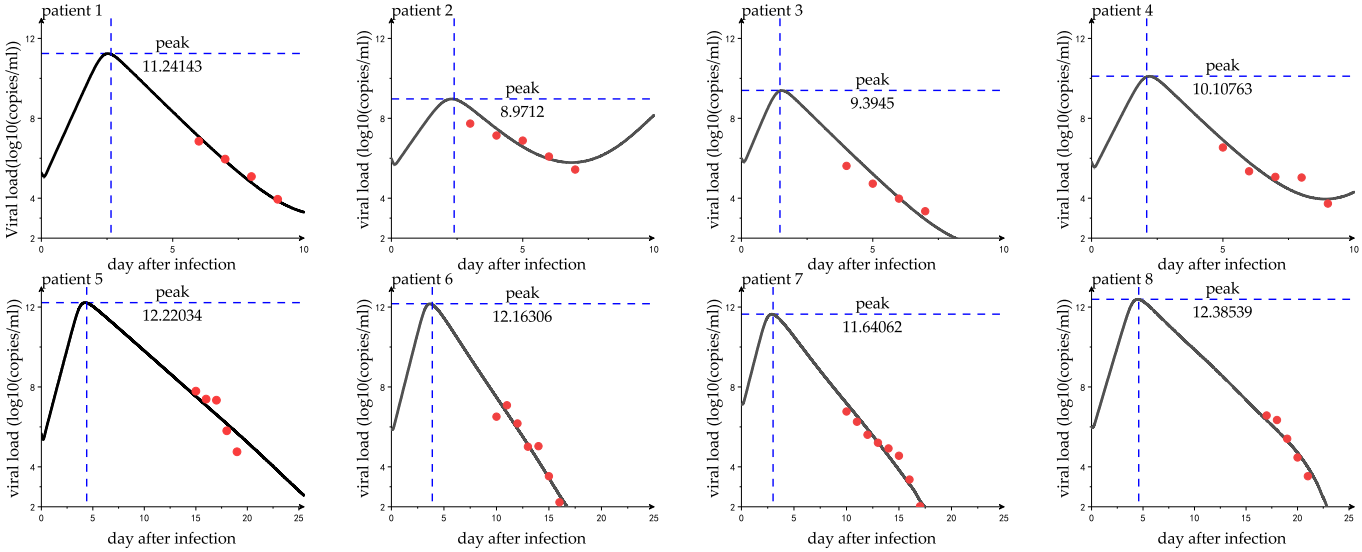


**Figure 4.** Dynamic changes in eight patients' viral loads: patients 1, 2, 3, and 4 are mild disease patients; patients 5, 6, 7, and 8 are severe disease patients. The peak viral load of mild patients (11.24, 8.97, 9.39, 10.11) is greater than that of severe patients (12.22, 12.16, 11.64, 12.39), and the viral load of mild patients peaks earlier than that of severe patients.

**Table 3.** Some parameter values in Model 1 and Model 2.

| | $\beta$ | $p$ | $\delta_I$ | $c$ | $V_0$ | $R_0$ |
|---|---|---|---|---|---|---|
| Patient 1 | 0.054 | $1.45 \times 10^5$ | 13.90 | 11.93 | $1.87 \times 10^{-4}$ | 2.48 |
| Patient 2 | 4.28 | $1.37 \times 10^3$ | 18.02 | 12.71 | $9.67 \times 10^{-4}$ | 1.85 |
| Patient 3 | 3.80 | $3 \times 10^3$ | 19.12 | 13.26 | $9.74 \times 10^{-4}$ | 2.46 |
| Patient 4 | 0.58 | $1.23 \times 10^4$ | 13.20 | 13.95 | $6.56 \times 10^{-4}$ | 2.29 |
| Mean | 2.18 | $4.04 \times 10^4$ | 16.06 | 12.96 | $6.69 \times 10^{-4}$ | 2.27 |
| Patient 5 | $7.24 \times 10^{-3}$ | $1.49 \times 10^5$ | 1.03 | 7.76 | $4.55 \times 10^{-4}$ | 4.13 |
| Patient 6 | $7.74 \times 10^{-3}$ | $1.68 \times 10^5$ | 7.28 | 1.74 | $7.61 \times 10^{-4}$ | 2.79 |
| Patient 7 | $3.07 \times 10^{-2}$ | $3.19 \times 10^4$ | 4.94 | 1.42 | $1.39 \times 10^{-2}$ | 3.06 |
| Patient 8 | $4.60 \times 10^{-3}$ | $1.36 \times 10^5$ | 4.21 | 1.05 | $9.66 \times 10^{-4}$ | 2.81 |
| Mean | $1.26 \times 10^{-2}$ | $1.22 \times 10^5$ | 4.36 | 2.99 | $4.01 \times 10^{-3}$ | 3.20 |

Patient 1, 2, 3, and 4 are mild patients; Patient 5, 6, 7, and 8 are severe patients.

Parameter $\beta$ reflects the intensity of the effect of the viral infection on healthy cells. This is generally affected by two aspects: the infection mechanism of the virus itself is affected by the affinity of receptors on healthy cells and the cells' antiviral mechanism also exerts a great influence. Smoking and some drugs for other diseases may upregulate the activity of the receptor [36]. Viruses can evade immunity by enhancing viral adhesion and increasing the viral invasion [37]. Interferons can prevent viruses from infecting healthy cells [38]. At the initial stage of the virus entering the human body, the immunocyte-like plasma dendritic cells (pDC) secrete massive concentrations of interferons [3]. The $\beta$ of severe disease patients is significantly lower than that of mild disease patients, indicating

that, in the late stage of the immune response, the severe disease patients probably retain a higher level of interferons, which has a negative influence on normal cell function. Medical research shows that COVID-19 patients with severe disease often have high concentrations of interferons and cytokines, mainly protein interleukin 6 (IL-6), which renders the cytokine storm, and causes functional damage to the body [3]. In terms of clinical treatment, there is a corresponding new treatment method involving the injection of an IL-6 inhibitor [24]. Generally, the $\beta$ value distribution of severe disease patients is much more concentrated (Figure 5A), signifying that the unstable generation of interferons is common for severe patients.

Parameter $p$ reflects the rate at which cells break down to produce viruses. Generally, patients with severe disease have higher $p$ values. This signifies that SARS-CoV-2 RNA in the cells of severe disease patients can be better replicated and might expresses an immune escape mechanism such as affecting cells' antiviral state by using specified proteins [37,38] different from those used in mild disease patients. On one hand, interferons can reduce viral infection in cells, and on the other hand, they can reduce viral replication in cells. Severe disease patients have low $\beta$ values but high $p$ values, which signifies that, in severe disease patients, they have a limited impact on viral replication. In clinical treatment studies, the impact of interferons on viral replication can be studied. Overall, mild and severe disease patients have overlapping values, but there is a more concentrated distribution of severe patients (Figure 5B), which indicates that while some mild patients have these effects but they are more common in severe disease patients.

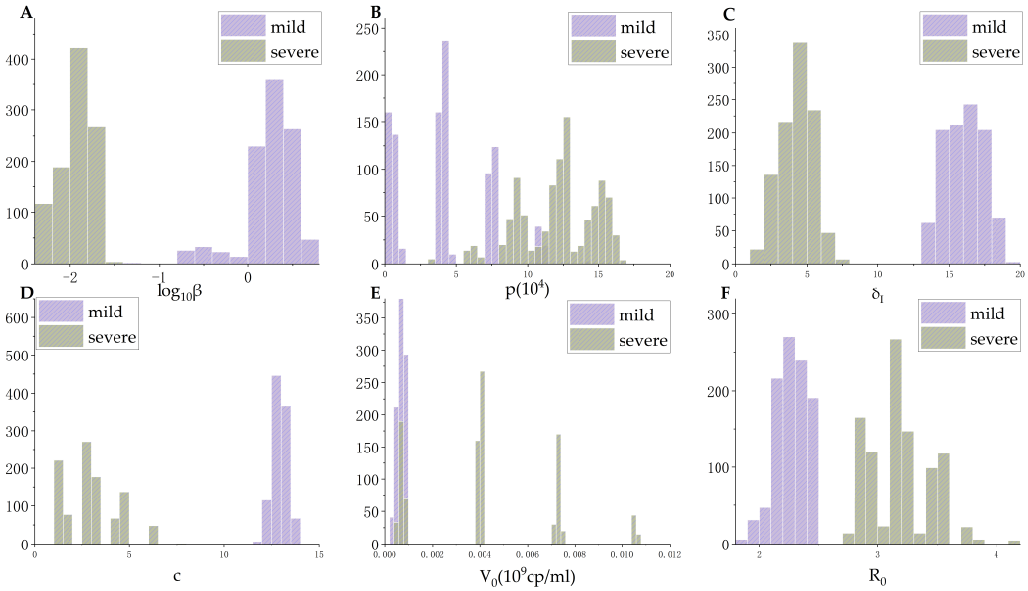


**Figure 5.** Bootstrap sampling distribution of Model 1 parameters. (**A**) $\log_{10}\beta$; (**B**) $p$; (**C**) $\delta_I$; (**D**) $c$; (**E**) $V_0$; (**F**) $R_0$. The kurtosis of $\beta$, $p$, $\delta_I$, $V_0$, $R_0$ of mild patients is $-0.54, 0.53, -0.13, 0.0011, -0.23, -0.46$; the kurtosis of severe patients is $-0.222, -0.15, -0.22, -0.19, -0.36, -0.05$. Kurtosis can reflect the concentration of data around the mean: the higher the kurtosis is, the greater the concentration is. The distribution of each parameter was found to be significantly different between patients with mild and severe disease using the Mann–Whitney test ($p$-value $< 1$).

Parameter $\delta_I$ indicates the death of infected cells other than T cells and allows us to consider the killing effect of NK cells or the apoptosis induced by other immune cells [3]. Severe disease patients were shown to have cells with a lower killing effect than mild disease patients, which is consistent with medical studies. For instance, NK cells in severe disease patients are suppressed by the cytokine storm [3]. Overall, the $\delta_I$ value distribution of severe disease patients is more concentrated than in mild disease patients, and the distribution of the two is quite different.

Parameter $c$ indicates the inactivation of free viruses by cells other than antibodies, such as the killing of viruses by neutrophil extracellular traps (NETs), macrophage phagocytosis of cells, and so on. The c value of mild disease patients is significantly higher than that of severe ones, possibly because immune cells are inhibited to varying degrees. For instance, the NET reaction leads to the pyroptosis of macrophages [3], and macrophages can transmit information to promote T cell maturation, which affects the initiation of adaptive immunity [38]. Overall, the concentration of $c$ values in mild and severe disease patients is comparable, while the distributions of the two are quite different (Figure 5D), which indicates that these processes are common in severe disease patients but rarely occur in mild disease patients.

$V_0$ indicates patients' initial viral load, and severe disease patients have a higher initial viral load than mild disease patients, which means that severe disease patients not only have a higher viral load in the middle and late stages of viral infection [39], but also inhale more viruses in the early stages. Mild disease patients have a more concentrated overall distribution (Figure 5E). At the same time, a relatively low level of viral infection occurs in the initial stage for severe disease patients. This signifies that, in the early stages of infection, potential severe disease patients inhale SARS-CoV-2 more easily, and although there is the possibility of relatively low inhalation, there is a strong onset of illness due to differences in the immune system.

Generally, although the difference in the basic reproduction number $R_0$ is relatively small between severe and mild disease patients, it can be used to differentiate severe and mild disease patients. To provide better clinical guidance, we classified patients with different $R_0$ values into severe and mild disease $\alpha$ quantiles. By calculating the quantile of the bootstrap sample from Figure 5F, we determined that because the proportion of moderate to severe patients accounted for 20% [40] of all patients, mild and severe disease patients accounted for $\alpha$ = 80% and $\alpha$ = 20% of all patients, respectively, giving basic reproduction values of 2.39 and 2.93, respectively. That is, patients with a basic reproduction number of less than 2.39 have an 80% probability of developing mild disease, and patients with a basic reproduction number of more than 2.93 have an 80% probability of developing severe disease. We provide the classification of patients in (Figure 6). It should be emphasized that the selection of quantiles is not fixed; they should be selected by integrating factors such as epidemic prevention and the economic conditions. We intend to provide a feasible method to distinguish mild disease patients, severe disease patients, and at-risk patients that does not rely on clinical symptoms. Doing so, on the one hand, could avoid excessive occupation of medical resources and, on the other hand, could better identify at-risk patients so that they can receive increased attention.

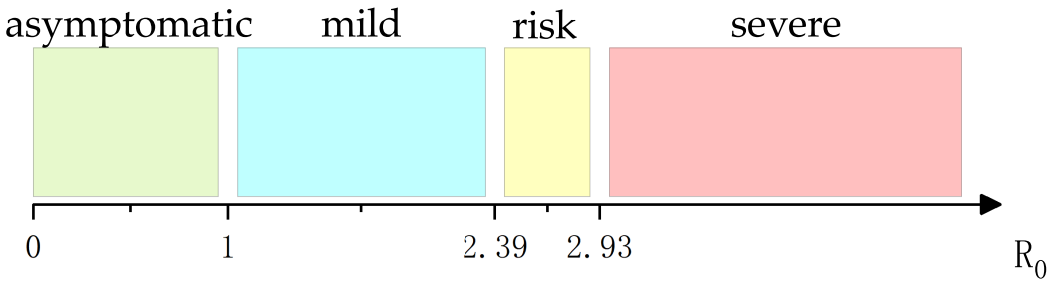


**Figure 6.** Classification of patients based on basic reproduction number. If $R_0 \leq 1$, the patient is asymptomatic. If $1 \leq R_0 < 2.39$ ,the patient is mild. If $2.39 \leq R_0 < 2.93$ , the patient is at risk of becoming severe. If $R_0 \geq 2.93$, the patient is severe. Patients at risk of mild to severe disease should be focused on.

Both antibody clearance of viruses and the killing effect of T cells on infected cells are indispensable to human immunity. Here, based on the calculation formula for the basic reproduction number (14), we suppose that $\delta_I = \sigma_G = \sigma_M = 0$ can be used to simulate change of basic reproduction number in the absence of adaptive immunity (Figure 7).

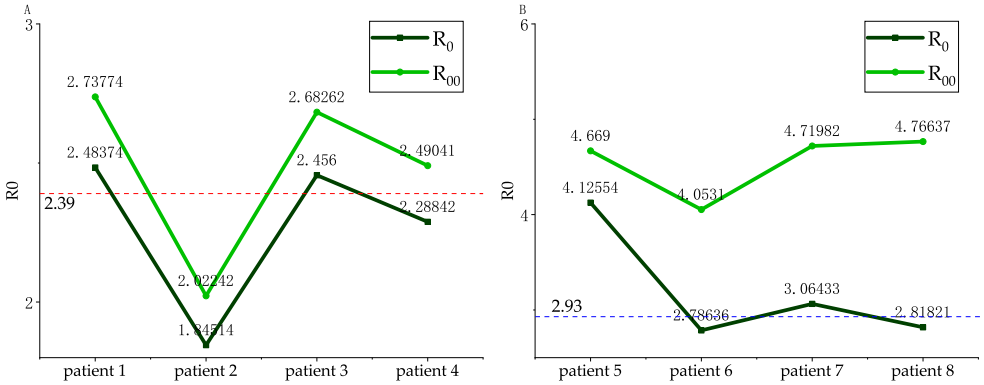


**Figure 7.** With the basic reproduction number ($R_0$) and without T cells and antibodies ($R_{00}$): (**A**) mild patients; (**B**) severe patients. The red line indicates the boundary between at-risk and mild patients. The blue line indicates the boundary between at-risk and severe patients.

According to the patient classification given in this paper (Figure 6), when the roles of the T cells and antibodies are lost, patient 4 changes from a mild disease to an at-risk patient (Figure 7A), and the corresponding medical treatment is required; patients 6 and 8 are converted from at-risk patients to severe disease patients (Figure 7B). The non-immune basic reproduction number ($R_{00}$) in all patients increases, and the growth rate in severe disease patients is greater ($R_0 - R_{00}$). This suggests that patients with severe disease are more dependent on their immune capacity, although their immune capacity is relatively more unstable.

Overall, the basic reproduction number $R_0$ is a relatively good tool to evaluate the infectivity of the virus in the human body. Although the difference is small, severe disease patients generally have higher $R_0$ values than mild disease patients. We can also take $R_0$ as the standard to distinguish mild and severe disease patients. The reason for severe and mild disease patients having different $R_0$ values is that mild disease patients always have a more stable antiviral effect and a stronger ability to kill viruses and infected cells. The triggers for severe illness come from viral infection and excessive activation of immunity. Although severe disease patients do not have good immunity, they are more dependent on T cells and antibodies than mild disease patients. Clinically, when the classification criteria of patients given in this paper are used for different patients, particularly for at-risk patients, the right medicine can be prescribed and the corresponding treatment provided.

### *3.2. T Cells Delay and Treatment Regimen*

After being infected by a virus, infected cells secrete cytokines, and immature T cells gradually differentiate with some time delay. Since adaptive immunity is more efficient, severe disease patients show later detection of antibodies and T cells. We simulated this process using Model 2. The parameter estimates are shown in Table 4 and the distribution is shown in Figure 8.

**Table 4.** Some parameter values in Model 2.

| | $\omega$ | $\tau$ | $\delta_T$ | | $\omega$ | $\tau$ | $\delta_T$ |
|---|---|---|---|---|---|---|---|
| Pt 1 | 0.031 | 1.85 | 0.015 | Pt 5 | $1.18 \times 10^{-4}$ | 10.95 | 0.026 |
| Pt 2 | 0.038 | 1.28 | 0.066 | Pt 6 | $6.38 \times 10^{-4}$ | 12.43 | 0.024 |
| Pt 3 | 0.042 | 2.82 | 0.014 | Pt 7 | $4.13 \times 10^{-4}$ | 13.50 | 0.023 |
| Pt 4 | 0.029 | 1.30 | 0.030 | Pt 8 | $4.71 \times 10^{-4}$ | 11.16 | 0.026 |
| Mean | 0.025 | 1.81 | 0.031 | Mean | $4.10 \times 10^{-4}$ | 12.01 | 0.025 |

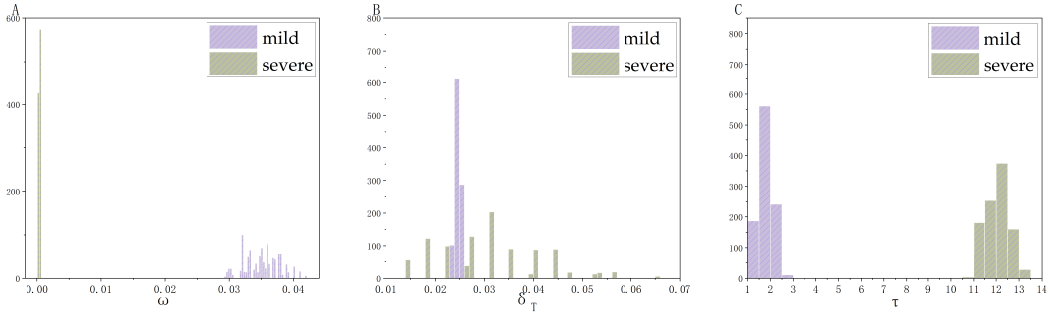


**Figure 8.** Bootstrap sampling distribution of Model 2 parameters: (**A**) $\omega$; (**B**) $\delta_T$; (**C**) $\tau$; The kurtosis of $\omega$, $\delta_T$, $\tau$ of severe patients is $-0.61$, $-0.42$, and $-0.41$; the kurtosis of mild patients is $-0.29$, 0.062, and 10.95. The distribution of each parameter was found to be significantly different between patients with mild and severe disease using the Mann–Whitney test ($p$-value $< 1$).

On average, the recruitment rate of infected cells to T cells in mild patients was found to be 0.025, higher than the value of 0.00041 found for severe patients, while the T cell clearance was shown to be greater than in severe patients. However, after observing every patient, we found that except for patient 2, all patients had relatively low clearance of T cells. New mature T cells appeared in severe disease patients after an average of 12.01 days, while in mild disease patients, T cells only took an average of 1.81 days to appear. The main factor contributing to the difference between severe and mild disease patients is the adaptive immune delay time, i.e., the complete maturation time of T cells. Overall, the recruitment rate and clearance rate of T cells were found to be more concentrated in severe disease patients, showing that severe disease patients have low recruitment of T cells and weak clearance of T cells. All mild disease patients had a T cell delay time of less than 3 days, while severe disease patients had a T cell delay time of more than 10 days. Thus, intensive care is required by all clinically available patients who have not produced large amounts of T cells on the first day after the appearance of symptoms, i.e., three days after infection.

The viral load of severe disease patients is usually higher than that of mild disease patients [39], which can also be used as the criteria for evaluating disease changes. In clinical treatment, general treatment of mild patients is generally undertaken first, i.e., bed rest, detection of vital signs, oxygen treatment, and so on. For severe disease patients, drug treatment can be adopted [24]. We assumed that on the day of symptom appearance, i.e., the second day after infection, general treatment was given to patients, and the duration of medication was dependent on the situation. The effect of different treatments with an average viral load of seven days was described. Drug treatment can reduce the viral load of patients [41]. An animal experiment showed that the effect of reducing the viral load is related to the drug dosage, and it was proven that some drugs, such as massetini, can reduce the viral load by more than 99% [42]. Hyperbaric oxygen therapy can reduce the viral load, so changes in the viral load are often used to observe the effect of treatment [43].

In summary, based on a reasonable analysis, we assume that general treatment reduces the viral load by 50%, and drug treatment reduces it by 90%. We used representative severe and mild disease patients, i.e., the mean values of parameters from Model 2 to describe the medical process.

Whether drug treatment or general treatment is used, for mild disease patients, the viral load decreases every day, and the effect of drug treatment is more obvious (Figure 9A). However, for severe disease patients, if medication is taken the day after viral infection, the viral load rises again after a period of decline (Figure 9B), showing that this drug treatment start time is not the best for mild disease patients. If drug treatment is taken on the third day after infection, i.e., combined treatment, the viral load will decline significantly.

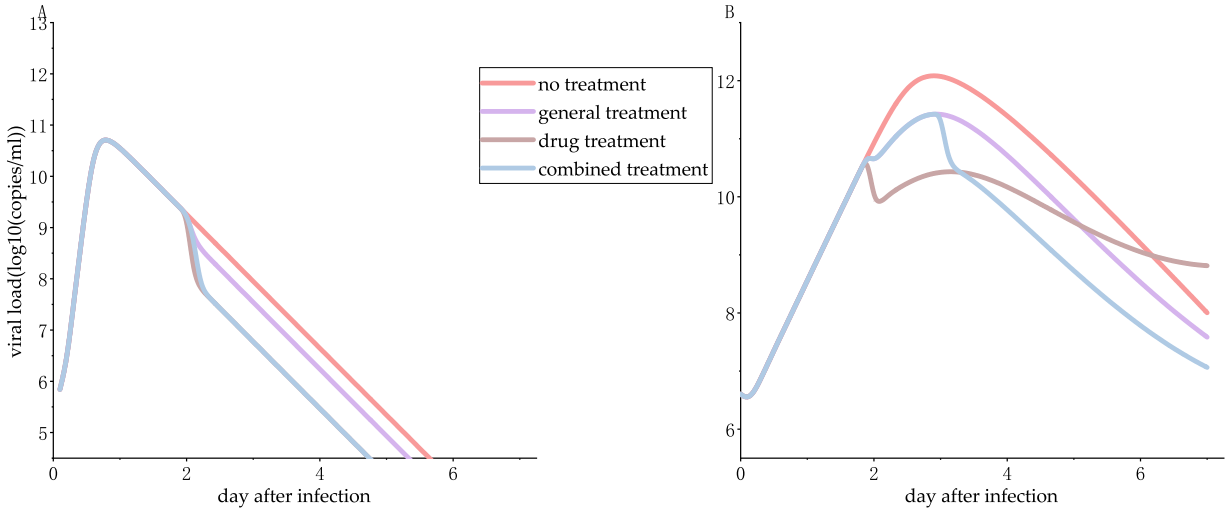


**Figure 9.** Changes in the viral load without treatment and following general treatment, drug treatment, and combined treatment: (**A**) mild patients (combined treatment refers to general treatment and drug treatment starting the day after infection); (**B**) severe patients (combined treatment refers to general treatment starting the day after infection and drug treatment starting the third day after infection).

For mild patients, general treatment reduces the viral load by 0.293, and drug treatment reduces the viral load by 0.846. Early drug treatment has a better ability to reduce the viral load (Figure 10). In severe patients, general treatment reduces the viral load by 0.463, and drug treatment reduces it by 0.602. Combined treatment, i.e., taking drug treatment on the third or fourth day after infection, better reduces the average viral load of a week, i.e., better efficacy.

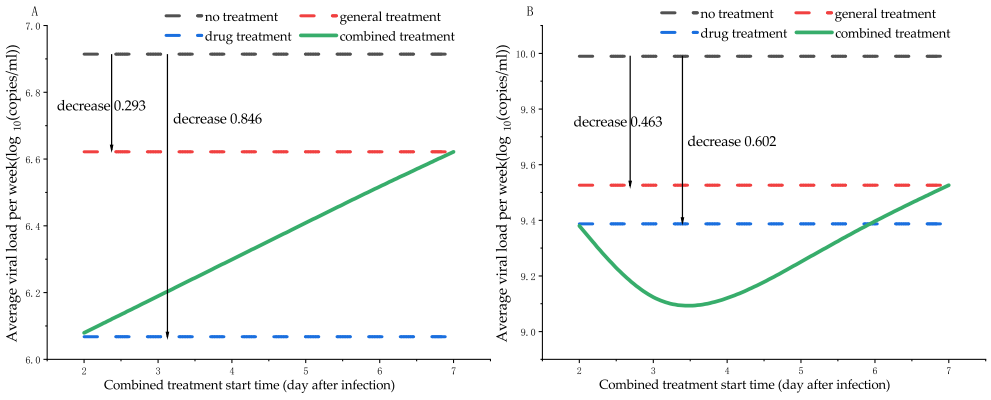


**Figure 10.** Relationship between the drug treatment start time and the average viral load in a week with combined treatment: (**A**) mild patients (the average viral load increased after delayed drug treatment); (**B**) severe patients (the average viral load decreased first and then increased with the onset of drug treatment)

Overall, the third day after infection is the best time for combined treatment of potential severe disease patients, and T-cells generally appear in the bodies of severe disease patients after the third day. As a result, the detection of T cells in vivo should be done when a patient has symptoms. If the value is lower than $2 \times 10^5$ cells/mL, drug treatment should be initiated (Figure 11). We suggest that the content of T cells should be detected, and the treatment plan should be adjusted in a timely and accurate manner with clinical examination.

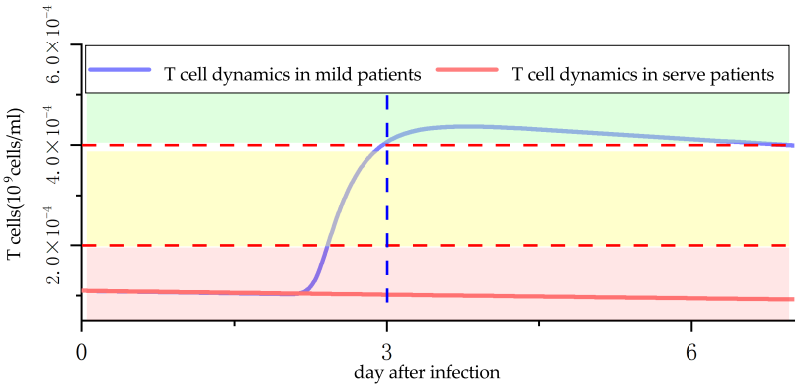


**Figure 11.** T cell changes in mild and severe disease patients without treatment. The T cell concentration is measured on the third day, and if the value is lower than $2 \times 10^5$ cells/mL (red part), drug treatment should be administered the same day; if it is higher than $2 \times 10^5$ cells/mL and lower than $4 \times 10^5$ cells/mL (yellow part), more clinical information should be used to determine whether drug treatment is needed; if it is higher than $4\times10^5$ cells/mL (green part), general treatment should be continued.

## 4. Discussion

In this paper, SARS-CoV-2 was taken as the research object, and the viral kinetic model was used to simulate the infection mechanism of COVID-19 and the human immune system. Additionally, the immune difference between mild and severe disease patients was analyzed and compared in an attempt to give clinical explanations for the results and further provide clinical suggestions. Two main research methods were used, and the results are as follows: First, by constructing Model 1 to estimate the basic reproduction number and specific parameters of other models, it was found that the basic reproduction number of severe disease patients is generally greater than that of patients with mild symptoms, but the difference is small. The reason for the difference in $R_0$ is the different response characteristics of patients' immune systems. A classification method for patients was proposed based on the distribution of $R_0$. Secondly, Model 2 was constructed to function as an effective tool to estimate and calculate the maturation time of T cells. Studies have shown that the maturation time of T cells is longer in severe disease patients, which is consistent with clinical medical results. Combining the two points, it appears to be the difference in immune system characteristics that determines whether a patient has severe or mild symptoms, and this can be used to provide different clinical treatment suggestions for different patients. This paper suggests that, in terms of personal protection, it is important to enhance one's own resistance. In terms of the prevention and control of the epidemic, it is recommended, where possible, to apply more stringent epidemic prevention mechanisms to the population with poor immune capacity. In terms of clinical treatment, corresponding treatments can be given according to T cell observations.

Compared with similar studies [17], this paper has some similarities and differences. Similar to previous studies, we distinguished different types of research objects and analyzed the differences based on the viral infection model. The results show that different immune abilities are the main cause of the differences between research objects. Some previous studies used laboratory animals rather than actual patients, which may be due to a relative lack of data. This study used real patient data, making the results more consistent with clinical results. The data, however, are relatively scarce and difficult to obtain, so the sample size used in this study was small, and the parameter distribution given may not be accurate.

Some shortcomings also exist. First of all, the data on the viral load used in this study were no different in terms of sampling, but the difference in results was possibly caused by different methods of sampling [17]. Additionally, in this study, relatively few data were used, and the sample size was small, so our results may differ from the overall results. In

the context of the COVID-19 pandemic, more comprehensive data are desired to ensure that the results are objective and reasonable.

## 5. Conclusions

SARS-CoV-2 infects different people with different levels of severity. The basic reproduction number $R_0$ of severe disease patients is greater than that of mild disease patients. This is because, in severe disease patients, the immune system has a poor capacity to clear infected cells and free viruses. In addition, viruses can replicate more frequently in cells.

In this paper, we constructed two mathematical model to evaluate the infectivity of SARS-CoV-2 in patients with different disease levels. We used the first model to calculate the basic reproduction number and then classify severe and mild patients. The other model can be used to analyze and compare the delay time of T cell action in patients with different symptoms. For example, patients with $R_0$ less than 2.93 and greater than 2.39 may be identified as high-risk patients, 20% of which are severe patients. If the clinical symptoms of patients are mild at this time, they are advised to undergo clinical observation. T cells take longer to mature in severe disease patients, so they can be used as an early standard to determine the treatment plans of patients. The best time for severe patients to undergo drug treatment is on the third day after infection, i.e., the first day after the onset of symptoms. Therefore, more attention should be paid to patients who fail to show a high level of T cells, regardless of their clinical symptoms, to determine whether a combination of drugs and general treatment is required as early as possible.

In future, we will introduce some thresholds with statistical characteristics to further characterize the impact of the uncertainty of incubation period on virus transmission [44], and explore expression and replication of virus genes at the single cell level [45] and the multi-scale modeling of gene random expression and virus transmission [46].

**Author Contributions:** Conceptualization, Y.Y. and Q.S.; methodology, Y.Y.; software, Y.Y.; validation, Y.Y. and Q.S.; formal analysis, Y.Y.; investigation, Y.Y.; resources, Y.Y.; data curation, Y.Y.; writing—original draft preparation, Y.Y., C.X. and Y.X.; writing—review and editing, Y.Y., C.X. and Y.X.; visualization, Y.Y.; supervision, Y.Y., C.X. and Y.X.; project administration, Q.S.; funding acquisition, Q.S. All authors have read and agreed to the published version of the manuscript.

**Funding:** This work was supported by the National Natural Science Foundation of China (No. 12171113) and the Natural Science Foundation of Guangdong, China (No. 2022A1515010242).

**Institutional Review Board Statement:** Not applicable.

**Informed Consent Statement:** Not applicable.

**Data Availability Statement:** All data included in this study are available upon request by contact with the corresponding author.

**Acknowledgments:** Thank you to all the anounymos reviewers for their sincere suggestions. Thank you Hanying Bian for your encouragement to the author Yingdong Yin.

**Conflicts of Interest:** The authors declare no conflict of interest.

## References

1. Weekly Epidemiological Update on COVID-19-1 June 2022. Available online: https://www.who.int/publications/m/item/weekly-epidemiological-update-on-covid-19---1-june-2022 (accessed on 8 May 2022).
2. Xu, Y.H.; Dong, J.H.; An, W.M.; Lv, X.Y.; Yin, X.P.; Zhang, J.Z.; Dong, L.; Ma, X.; Zhang, H.J.; Gao, B.L. Clinical and computed tomographic imaging features of novel coronavirus pneumonia caused by SARS-CoV-2. *J. Infect.* **2020**, *80*, 394–400. [CrossRef]
3. Paludan, S.; Mogensen, T. Innate immunological pathways in COVID-19 pathogenesis. *Sci. Immunol.* **2022**, *7*, abm5505. [CrossRef]
4. Sette, A.; Crotty, S. Adaptive immunity to SARS-CoV-2 and COVID-19. *Cell* **2021**, *184*, 861–880. [CrossRef]
5. Yoshida, S.; Ono, C.; Hayashi, H.; Fukumoto, S.; Shiraishi, S.; Tomono, K.; Arase, H.; Matsuura, Y.; Nakagami, H. SARS-CoV-2-induced humoral immunity through B cell epitope analysis in COVID-19 infected individuals. *Sci. Rep.* **2021**, *11*, 5934. [CrossRef]
6. Nowak, M.A.; Bonhoeffer, S.; Hill, A.M.; Boehme, R.; Thomas, H.C.; McDade, H. Viral dynamics in hepatitis B viral infection. *Proc. Natl. Acad. Sci. USA* **1996**, *93*, 4398–4402. [CrossRef]

7. Li, M.; Xu, F.; Huang, J.; Li, L.; Yang, J.; Xu, L.; He, Y.; Zheng, Q.; Wang, K. Research and evaluation of virus dynamic model. *Clin. Pharmacol. Ther. China* **2016**, *21*, 653–660.
8. Perelson, A. Modelling viral and immune system dynamics. *Nat. Rev. Immunol.* **2002**, *2*, 28–36. [CrossRef]
9. Baccam, P.; Beauchemin, C.; Macken, C.A.; Hayden, F.G.; Perelson, A.S. Kinetics of influenza A viral infection in humans. *J. Virol.* **2006**, *80*, 7590–7599. [CrossRef]
10. Li, B.; Jiao, F. A delayed HIV-1 model with cell-to-cell spread and virus waning. *J. Biol. Dyn.* **2020**, *14*, 802–825. [CrossRef]
11. Miao, H.; Hollenbaugh, J.A.; Zand, M.S.; Holden-Wiltse, J.; Mosmann, T.R.; Perelson, A.S.; Wu, H.; Topham, D.J. Quantifying the early immune response and adaptive immune response kinetics in mice infected with influenza A virus. *J. Virol.* **2010**, *84*, 6687–6698. [CrossRef]
12. Nowak, M.A.; Bonhoeffer, S.; Shaw, G.M.; May, R.M. Anti-viral drug treatment: Dynamics of resistance in free virus and infected cell populations. *J. Theor. Biol.* **1997**, *184*, 203–217. [CrossRef] [PubMed]
13. Rong, L.; Ribeiro, R.; Perelson, A. Modeling quasispecies and drug resistance in hepatitis C patients treated with a protease inhibitor. *Bull. Math. Biol.* **2012**, *74*, 1789–1817. [CrossRef] [PubMed]
14. Pawelek, K.A.; Huynh, G.T.; Quinlivan, M.; Cullinane, A.; Rong, L.; Perelson, A.S. Modeling within-host dynamics of influenza viral infection including immune responses. *PLoS Comput. Biol.* **2012**, *8*, e1002588. [CrossRef] [PubMed]
15. Alimohamadi, Y.; Taghdir, M.; Sepandi, M. Estimate of the basic reproduction number for COVID-19: A systematic review and meta-analysis. *J. Prev. Med. Public Health* **2020**, *53*, 151. [CrossRef] [PubMed]
16. Gonçalves, A.; Maisonnasse, P.; Donati, F.; Albert, M.; Behillil, S.; Contreras, V.; Naninck, T.; Marlin, R.; Solas, C.; Pizzorno, A.; et al. SARS-CoV-2 viral dynamics in non-human primates. *PLoS Comput. Biol.* **2021**, *17*, e1008785. [CrossRef]
17. Rodriguez, T.; Dobrovolny, H. Estimation of viral kinetics model parameters in young and aged SARS-CoV-2 infected macaques. *R. Soc. Open Sci.* **2021**, *8*, 202345. [CrossRef]
18. Vaidya, N.; Bloomquist, A.; Perelson, A. Modeling within-Host dynamics of SARS-CoV-2 infection: A case study in Ferrets. *Viruses* **2021**, *13*, 1635. [CrossRef]
19. Wang, S.; Pan, Y.; Wang, Q.; Miao, H.; Brown, A.N.; Rong, L. Modeling the viral dynamics of SARS-CoV-2 infection. *Math. Biosci.* **2020**, *328*, 108438. [CrossRef]
20. Goyal, A.; Cardozo-Ojeda, E.; Schiffer, T. Potency and timing of antiviraltherapy as determinants of duration of SARS-CoV-2 shedding and intensity of inflammatory response. *Sci. Adv.* **2020**, *6*, eabc7112. [CrossRef]
21. Jenner, A.L.; Aogo, R.A.; Alfonso, S.; Crowe, V.; Deng, X.; Smith, A.P.; Morel, P.A.; Davis, C.L.; Smith, A.M.; Craig, M. COVID-19 virtual patient cohort suggests immune mechanisms driving disease outcomes. *PLoS Pathog.* **2021**, *17*, e1009753. [CrossRef]
22. Blanco-Rodríguez, R.; Du, X.; Hernández-Vargas, E. Computational simulations to dissect the cell immune response dynamics for severe and critical cases of SARS-CoV-2 infection. *Comput. Methods Programs Biomed.* **2021**, *211*, 106412. [CrossRef] [PubMed]
23. Néant, N.; Lingas, G.; Le Hingrat, Q.; Ghosn, J.; Engelmann, I.; Lepiller, Q.; Gaymard, A.; Ferré, V.; Hartard, C.; Plantier, J.C.; et al. Modeling SARS-CoV-2 viral kinetics and association with mortality in hospitalized patients from the French COVID cohort. *Proc. Natl. Acad. Sci. USA* **2021**, *118*, e2017962118. [CrossRef] [PubMed]
24. The General Office of the National Health Commission. COVID-19 Diagnosis and Treatment Program (Trial Version 9). Available online: http://www.nhc.gov.cn/cms-search/downFiles/ef09aa4070244620b010951b088b8a27.pdf (accessed on 8 May 2022).
25. Liu, Y.; Yan, L.M.; Wan, L.; Xiang, T.X.; Le, A.; Liu, J.M.; Peiris, M.; Poon, L.L.; Zhang, W. Viral dynamics in mild and severe cases of COVID-19. *Lancet Infect. Dis.* **2020**, *20*, 656–657. [CrossRef]
26. Miranda, R.L.; Guterres, A.; de Azeredo Lima, C.H.; Niemeyer Filho, P.; Gadelha, M.R. Misinterpretation of viral load in COVID-19 clinical outcomes. *Virus Res.* **2021**, *296*, 198340. [CrossRef]
27. Marot, S.; Calvez, V.; Louet, M.; Marcelin, A.G.; Burrel, S. Interpretation of SARS-CoV-2 replication according to RT-PCR crossing threshold value. *Clin. Microbiol. Infect.* **2021**, *27*, 1056–1057. [CrossRef]
28. Han, M.S.; Byun, J.H.; Cho, Y.; Rim, J.H. RT-PCR for SARS-CoV-2: Quantitative versus qualitative. *Lancet Infect. Dis.* **2021**, *21*, 165. [CrossRef]
29. Killingley, B.; Mann, A.J.; Kalinova, M.; Boyers, A.; Goonawardane, N.; Zhou, J.; Lindsell, K.; Hare, S.S.; Brown, J.; Frise, R.; et al. Safety, tolerability and viral kinetics during SARS-CoV-2 human challenge in young adults. *Nat. Med.* **2022**, *28*, 1031–1041. [CrossRef]
30. Zhang, B.; Yue, D.; Wang, Y.; Wang, F.; Wu, S.; Hou, H. The dynamics of immune response in COVID-19 patients with different illness severity. *J. Med. Virol.* **2021**, *93*, 1070–1077. [CrossRef]
31. Kong, H. A Viral Dynamic Model Considering Immune Cell Self-Proliferation and Phased Generation. Master's Thesis, Southwestern University, Chongqing, China, 2020.
32. Bartholdy, C.; Christensen, J.P.; Wodarz, D.; Thomsen, A.R. Persistent viral infection despite chronic cytotoxic T-lymphocyte activation in gamma interferon-deficient mice infected with lymphocytic choriomeningitis virus. *J. Virol.* **2000**, *74*, 10304–10311. [CrossRef]
33. van den Driessche, P.; Watmough, J. Reproduction numbers and sub-threshold endemic equilibria for compartmental models of disease transmission. *Math. Biosci.* **2002**, *180*, 29–48. [CrossRef]
34. Chen, J.; Wu, H. Efficient local estimation for time-varying coefficients in deterministic dynamic models with applications to HIV-1 dynamics. *J. Am. Stat. Assoc.* **2008**, *103*, 369–384. [CrossRef]

35. Cevik, M.; Tate, M.; Lloyd, O.; Maraolo, A.E.; Schafers, J.; Ho, A. SARS-CoV-2, SARS-CoV, and MERS-CoV viral load dynamics, duration of viral shedding, and infectiousness: A systematic review and meta-analysis. *Lancet Microbe* **2021**, *2*, e13–e22. [CrossRef]
36. Jackson, C.B.; Farzan, M.; Chen, B.; Choe, H. Mechanisms of SARS-CoV-2 entry into cells. *Nat. Rev. Mol. Cell Biol.* **2022**, *23*, 3–20. [CrossRef]
37. Gu, W.; Gan, H.; Ma, Y.; Xu, L.; Cheng, Z.J.; Li, B.; Zhang, X.; Jiang, W.; Sun, J.; Sun, B.; et al. The molecular mechanism of SARS-CoV-2 evading host antiviral innate immunity. *Virol. J.* **2022**, *19*, 49. [CrossRef]
38. Cao, X. *Medical Immunology*; People's Health Press: Beijing, China, 2018.
39. Zheng, S.; Fan, J.; Yu, F.; Feng, B.; Lou, B.; Zou, Q.; Xie, G.; Lin, S.; Wang, R.; Yang, X.; et al. Viral load dynamics and disease severity in patients infected with SARS-CoV-2 in Zhejiang province, China, JanuaryMarch 2020: Retrospective cohort study. *BMJ* **2020**, *369*, m1443. [CrossRef] [PubMed]
40. Kaswa, R.; Govender, I. Novel coronavirus pandemic: A clinical overview. *S. Afr. Fam. Pract.* **2020**, *62*, a5123. [CrossRef]
41. Shao, Y.; Chen, J.; Lu, H. Update: Drug treatment options for coronavirus disease 2019 (COVID-19). *Biosci. Trends* **2021**, *15*, 345–349. [CrossRef]
42. Drayman, N.; DeMarco, J.K.; Jones, K.A.; Azizi, S.A.; Froggatt, H.M.; Tan, K.; Maltseva, N.I.; Chen, S.; Nicolaescu, V.; Dvorkin, S.; et al. Masitinib is a broad coronavirus 3CL inhibitor that blocks replication of SARS-CoV-2. *Science* **2021**, *373*, 931–936. [CrossRef]
43. Paganini, M.; Bosco, G.; Perozzo, F.A.; Kohlscheen, E.; Sonda, R.; Bassetto, F.; Garetto, G.; Camporesi, E.M.; Thom, S.R. The role of hyperbaric oxygen treatment for COVID-19: A review. *Med. Biomed. Updates* **2020**, *1289*, 27–35.
44. Jiao, F.; Tang, M. Quantification of transcription noise's impact on cell fate commitment with digital resolutions. *Bioinformatics* **2022**, *38*, 3062–3069. [CrossRef]
45. Chen, J.; Jiao, F. A novel approach for calculating exact forms of mRNA distribution in single-cell measurenments. *Mathematics* **2022**, *10*, 27. [CrossRef]
46. Wang, S.; Rong, L. Stochastic population switch may explain the latent reservoir stability and intermittent viral blips in HIV patients on suppressive therapy. *J. Theor. Biol.* **2014**, *360*, 137–148. [CrossRef]